

# Integrated Optical-Digital Approaches for Enhancing Image Restoration and Focus Invariance

V. P. Pauca<sup>a</sup>, R. J. Plemmons<sup>b</sup>, S. Prasad<sup>c</sup>, T. C. Torgersen<sup>a</sup>

<sup>a</sup>Department of Computer Science, Wake Forest University, Winston-Salem, NC 27109

<sup>b</sup>Department of Computer Science and Mathematics, Wake Forest University, Winston-Salem, NC 27019

<sup>c</sup>Center for Advanced Studies, University of New Mexico, Albuquerque, NM 87131

## ABSTRACT

A novel and successful optical-digital approach for removing certain aberrations in imaging systems involves placing an optical mask between an image-recording device and an object to encode the wavefront phase before the image is recorded, followed by digital image deconvolution to decode the phase. We have observed that when appropriately engineered, such an optical mask can also act as a form of preconditioner for certain deconvolution algorithms. It can boost information in the signal before it is recorded well above the noise level, leveraging digital restorations of very high quality. In this paper, we 1) examine the influence that a phase mask has on the incoming signal and how it subsequently affects the performance of restoration algorithms, and 2) explore the design of optical masks, a difficult nonlinear optimization problem with multiple design parameters, for removing certain aberrations and for maximizing restorability and information in recorded images.

**Keywords:** Pupil-phase mask, wavefront coding, integrated imaging, Fisher information, focus extension, image quality, image restoration, nonlinear optimization, pupil-phase engineering.

## 1. INTRODUCTION

In a recent paradigm, Dowski and Cathey<sup>1,2</sup> proposed the design of focus-invariant optical systems arrived at by means of designing the optics and the signal processing as an integrated imaging system. Specifically, they proposed the use of a cubic phase mask (see Eq. (9)) in the pupil of a standard, limited-focus imaging system to encode the wavefront of a three-dimensional object producing an intermediate image with spatially invariant blur by a known point spread function (PSF). Signal processing is then employed to digitally restore the intermediate image. Under suitable conditions, such restored images exhibit excellent depth-dependent detail. Without any phase encoding such detail would be washed out due to normal focus-dependent blur. The new integrated focus-invariant imaging systems can have more than an order of magnitude increase in depth of field.<sup>1</sup>

More recently, Prasad et al.<sup>3,4</sup> introduced the concept of *pupil-phase engineering* (PPE) to optimize the design of more general pupil-phase masks that can lead to even better performance than the cubic mask in extending depth of focus. Two PPE approaches were proposed that use the Strehl ratio (SR) and Fisher information (FI) as metrics of performance of such integrated optical-digital imaging systems. The SR is defined by the on-axis value of the PSF as a function of defocus. Candidate designs are pupil-phase masks that make the first few derivatives of the SR with respect to the defocus parameter be small without degrading the SR greatly. The FI metric uses the full PSF, not just its on-axis values, and measures the sensitivity of the PSF to defocus. Candidate designs lead to pupil-phase masks that minimize the FI metric, i.e. minimize the sensitivity of the PSF to defocus.

In this paper, we propose the design of pupil-phase masks that maximize restorability of the intermediate image by digital signal processing algorithms while minimizing sensitivity to defocus. Restorability is increased when a pupil-phase mask boosts information in the signal well above the noise level. The effect on digital algorithms includes faster convergence by iterative algorithms and, more importantly, much higher quality than what can be obtained through digital image restoration alone. Singular values and eigenvalues of the blurring

---

Send correspondence to V. P. Pauca: Email: paucavp@wfu.edu, Telephone: 1 336 758 5454

matrix are very effective when measuring restorability. We exploit the connection between these quantities and the optical transfer function (see Eq. (3)) and its magnitude, the modulation transfer function (see Eq. (4)) of an optical system. We consider restorability metrics that take in consideration the modulation transfer function over a finite range in the frequency domain, and employ the FI based metrics derived in previous work<sup>4</sup> to minimize sensitivity to defocus.

We first review basic concepts of Fourier optics, singular value and eigenvalue decomposition analysis of blurring matrices, as well as our PPE approaches to optimized pupil-phase masks based on the Strehl ratio and Fisher information. The joint problem of maximizing restorability while minimizing sensitivity to defocus is then posed. We consider two approaches. The first approach employs the restorability metric as an added penalty term to the nonlinear optimization problem resulting from the FI based formulation. The second employs a minimization-maximization approach that seeks to reduce variability of the MTF over a range of defocus. In the latter approach, we also consider representations of the phase in terms of Zernike polynomials. Computational results are presented for both approaches which include the optimized pupil-phase masks obtained as well as restoration results.

## 2. PRELIMINARIES

### 2.1. Fourier Optics

Within the PPE framework, consider phase functions  $\phi_\tau(\mathbf{x})$  of the form

$$\phi_\tau(\mathbf{x}) = \tau(x_1^2 + x_2^2) + \theta(\mathbf{x}), \quad (1)$$

where  $\mathbf{x} = (x_1, x_2)$  is a point in the pupil plane,  $\tau$  is the defocus parameter, and  $\theta(\mathbf{x})$  denotes higher order terms whose coefficients determine the shape of the pupil-phase mask. We henceforth refer to  $\theta(\mathbf{x})$  as the pupil mask function.

We define three relevant expressions related to  $\phi_\tau(\mathbf{x})$ : the point spread function (PSF), the optical transfer function (OTF), and modulation transfer function (MTF). For an incoherent imaging system, the PSF is proportional to the squared magnitude of the inverse Fourier transform of the generalized pupil function, i.e.

$$h(\boldsymbol{\omega}; \phi_\tau) = \left| \frac{1}{\lambda f \sqrt{A}} \iint P(\mathbf{x}) e^{i(\frac{2\pi}{\lambda f} \boldsymbol{\omega}^T \mathbf{x} + \phi_\tau(\mathbf{x}))} dx_1 dx_2 \right|^2. \quad (2)$$

In this expression,  $P(\mathbf{x})$  is the pupil function equal to 1 for all  $\mathbf{x}$  inside the pupil and 0 outside for a clear pupil,  $A$  is the area over the pupil,  $\lambda$  is the wavelength of illuminating light,  $f$  is the focal length, and  $\boldsymbol{\omega} = (\omega_1, \omega_2)$  is a point in the image plane. The OTF is the Fourier transform of the PSF,

$$H(\mathbf{u}; \phi_\tau) = \mathcal{F} \{h(\boldsymbol{\omega}; \phi_\tau)\}(\mathbf{u}), \quad (3)$$

where  $\mathbf{u} = (u, v)$  is a coordinate in the image frequency domain and  $\mathcal{F}$  is the two-dimensional Fourier transform. The MTF is the magnitude of the OTF,

$$M(\mathbf{u}; \phi_\tau) = |H(\mathbf{u}; \phi_\tau)|. \quad (4)$$

### 2.2. SVD and Ill-conditioning

The singular value decomposition (SVD) is an important tool for computation and for analysis of linear ill-posed problems. Consider a matrix  $A \in \mathbb{R}^{n \times n}$ . Then, the SVD of  $A$  is given by

$$A = U \Sigma V^T, \quad (5)$$

where  $\Sigma = \text{diag}(\sigma_1, \dots, \sigma_n)$  and  $U \in \mathbb{R}^{n \times n}$  and  $V \in \mathbb{R}^{n \times n}$  contain the left singular and right singular vectors of  $A$ , respectively.<sup>5</sup>  $U$  and  $V$  are orthonormal matrices and the singular values  $\sigma_i$  satisfy  $\sigma_1 \geq \sigma_2 \geq \dots \geq \sigma_n > 0$ , assuming  $A$  has rank  $n$ . The condition number of  $A$  is defined as  $\kappa(A) = \sigma_1/\sigma_n$ .

When  $A$  is a blurring operator defined by the PSF (see Eq. (2)) of an incoherent imaging system,  $\kappa(A)$  is very large. This is due to the well-known fact that digital image restoration is an ill-posed problem.<sup>6</sup> Small perturbations in the data lead to relatively large perturbation in the solution to linear systems involving  $A$ . In terms of (5), it is easy to see that such solutions involve  $\Sigma^{-1}$ : division by the small singular values magnify noise components corrupting the result.<sup>7,8</sup> This is a critical situation in image restoration problems where noise components are always present.<sup>9</sup>

The singular values of a circulant matrix  $C \in \mathbb{R}^{n \times n}$  can be computed using a discrete Fourier transform, i.e.  $\Sigma = \text{diag}(|F\mathbf{c}|)$ , where  $F$  is the  $n$ -by- $n$  Fourier transform matrix and  $\mathbf{c}$  is a column of  $C$ . Analogous results hold when  $C$  is block circulant with circulant blocks (BCCB). Circulant matrices are important in imaging as they arise naturally in numerical computations involving spatially invariant blur.<sup>9</sup>

We exploit an important connection between eigenvalues and singular values of circulant-type matrices and the OTF and MTF of an imaging system. In particular the eigenvalues of a BCCB matrix  $C \in \mathbb{R}^{n^2 \times n^2}$  are given by  $H(\mathbf{u}, \phi_\tau)$ . That is, for  $C = F\Lambda F$ , where  $\Lambda = \text{diag}(\lambda_1, \dots, \lambda_{n^2})$  and  $F$  is a 2-D Fourier transform matrix, the eigenvalues  $\lambda_i$  satisfy

$$\lambda_{in+j} = H((u_i, v_j); \phi_\tau), \quad i = 0 : n - 1, \quad j = 0 : n - 1. \quad (6)$$

Similarly, the singular values of  $C$  are given by  $M(\mathbf{u}, \phi_\tau)$ . That is, for  $C = U\Sigma V^T$ , the singular values  $\sigma_i$  satisfy

$$\sigma_{in+j} = M((u_i, v_j), \phi_\tau) = |\lambda_{in+j}|, \quad i = 0 : n - 1, \quad j = 0 : n - 1. \quad (7)$$

Moreover, by properties of the OTF, we have

$$\sigma_1 = M((0, 0), \phi_\tau) = 1. \quad (8)$$

For a circular pupil, the OTF has zero-crossings depending upon the value of the defocus parameter  $\tau$  and in general tends to decay at the high frequencies.<sup>9</sup> Correspondingly, the small singular values can be nearly or effectively zero, thus making  $\kappa(C)$  very large.

Next, we analyze the effect on restorability when the distribution of singular values of blurring matrices is altered via manipulation of the OTF and MTF as specified by formulas (6) and (7).

### 2.3. Restorability and Cubic Phase Elements

Restorability of an image is greatly affected by phase changes. These changes can have a significant impact in the quality of the restorations obtained by signal post-processing algorithms. We illustrate this point with cubic phase masks given by the following pupil mask function

$$\theta(\mathbf{x}) = \alpha(x_1^3 + x_2^3). \quad (9)$$

The parameter  $\alpha$  is the “strength” of the phase mask. As indicated earlier, cubic phase masks were originally proposed by Dowski and Cathey<sup>2</sup> and several of its properties have been studied by other authors.<sup>3,4,10</sup> We employ the connection between singular values and the MTF introduced earlier as well as the concepts of signal, transient, and noise subspaces used in digital image restoration.<sup>11</sup>

Let  $C(\tau, \alpha) \in \mathbb{R}^{n^2 \times n^2}$  with  $n = 1024$  denote a BCCB blurring matrix defined by the PSF in (2) as a function of  $\tau$  and  $\alpha$  with the phase given by (1) and (9). We consider the distribution of singular values of  $C(\tau, \alpha)$  over a range of  $\tau$  and  $\alpha$ .

For the special case of an object placed right at the plane of focus ( $\tau = 0$ ) and no cubic phase mask ( $\alpha = 0$ ), the MTF  $M(\mathbf{u}, \phi_0)$  is 1 at the origin and drops slowly toward zero as the frequencies increase. An on-axis cross-section of the MTF of such a system is illustrated by the triangular-shaped curve of Figure 1 (left). The corresponding singular values of  $C(0, 0)$  are relatively large in magnitude. A plot of singular values of  $C(0, 0)$  versus their magnitude is given by the curve labeled  $\alpha = 0, \tau = 0$  in Figure 1 (right). Incidentally, notice that even for this ideal case,  $\kappa(C(0, 0))$  is very large, as evident from the relative difference of the magnitudes of  $\sigma_1$  and  $\sigma_{n^2}$  in Figure 1 (right).

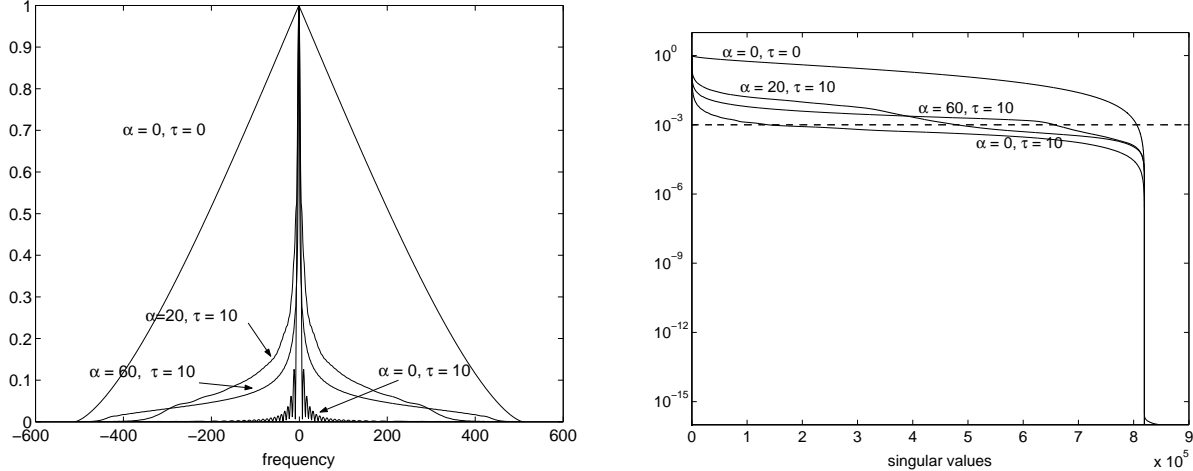


**Figure 1.** (left) On-axis cross-sections of the MTF for  $\tau = 0, 10$  and  $\alpha = 0, 20, 60$ . (right) Distribution of singular values of  $C(\tau, \alpha)$  for the same values of  $\tau$  and  $\alpha$ . Singular values above the dash-line constitute the signal subspace and those below the dash-line, the noise subspace.

In the case of a focusing error ( $\tau > 0$ ), defocus blur affects different parts of the image in proportion to the distance of different parts of the scene to the plane of focus. The larger the focusing error is, the lower the MTF. Figure 1 (left) shows the same cross-section of the MTF as before for a defocus amount given by  $\tau = 10$  and no cubic mask,  $\alpha = 0$ . Notice the sharp drop off toward zero near the origin. The corresponding singular values of  $C(10, 0)$  are significantly smaller in magnitude as illustrated in Figure 1 (right). Digital image restoration with  $C(10, 0)$  gives poor quality results even for relatively high signal-to-noise ratios. It is important to note that the magnitudes of the singular values cannot really be modified by digital means alone *after* the data has been collected. The quality of the data limits the quality of the solution.

In the case of negligible focusing error ( $\tau \approx 0$ ), a cubic phase element has the overall effect of lowering the MTF. However, for a large enough focusing error ( $\tau > 0$ ), the use of a cubic phase element can significantly raise the MTF relative to that of defocus only case. The curves for  $\alpha = 20$  and  $\alpha = 60$  in Figure 1 (left) illustrate this very important property. The singular values of  $C(10, 20)$  and  $C(10, 60)$  increase accordingly as shown in Figure 1 (right).

The effect of increasing the magnitude of the singular values via an optical element for defocus-type aberrations is a significant increase in the resolution of image restorations that can be obtained through post-processing. To see this we use the concepts of signal, noise and transient subspaces of Hanke, Nagy and Plemmons.<sup>11</sup> Suppose the data contains white Gaussian noise proportional to  $\epsilon$ . The signal subspace is given by the set  $\mathcal{S}$  of singular values greater than  $\epsilon$ , corresponding to components that are recoverable by post-processing. The noise subspace is given by the set  $\mathcal{N}$  of singular values less than  $\epsilon$ , corresponding to unrecoverable components corrupted by noise. The transient subspace is given by the set  $\mathcal{S} - \mathcal{N}$  corresponding to components that are near the noise level. As indicated by the dash-line in Figure 1 (right), for  $\epsilon = 10^{-3}$  there is over a factor of 3 gain in the dimension of the signal subspace as well a significant gain in magnitude for  $\alpha = 20$  and  $\alpha = 60$ . Components that were previously at or just below the noise level are now recoverable. This is important for restoration algorithms such as conjugate gradient type methods which iterate first through the signal space recovering the data. The iterations can be stopped before the noise begins to be magnified, a concept known as iterative regularization.

Based on these observations, we can formulate effective ways of measuring restorability for a given defocus parameter  $\tau$  and cubic phase strength  $\alpha$ . For example, we can define the metric

$$r_\tau(\alpha) = \sum_{i=1}^{n^2} \sigma_i(\tau, \alpha), \quad (10)$$

where  $\sigma_i(\tau, \alpha)$  denotes the dependence of the singular values on defocus error and strength of the cubic phase mask. Similar measures can be used that take in consideration the magnitude of the noise  $\epsilon$ . We refer to  $r_\tau(\alpha)$  as the restorability function for a given  $\tau$ . Plots of  $r_\tau(\alpha)$  for  $\tau = 0, 1, 3, 5, 7, 9, 11, 13, 15, 17, 19$  and  $\alpha \in [0, 60]$  are given Figure 2, illustrating the trade-off between restorability and insensitivity to defocus. Restorability as

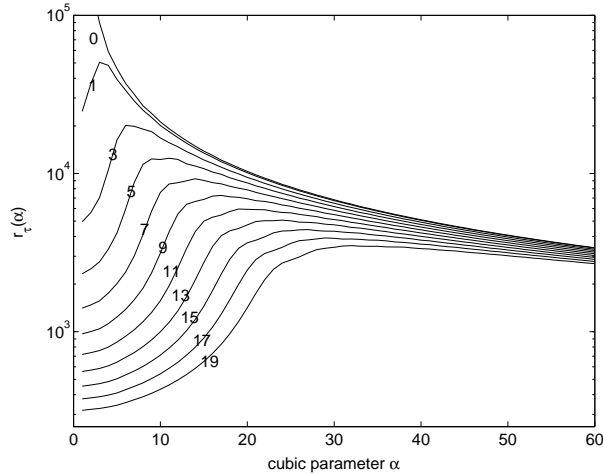


**Figure 2.** Restorability functions for the cubic pupil-phase mask.

measured by (10) bears resemblance to van der Gracht and Euliss<sup>10</sup> Shannon information theoretic analysis of cubic phase masks.

### 3. THE JOINT DESIGN PROBLEM

In this section we employ the relationship between the MTF and singular values to explore the joint problem of maximizing restorability while minimizing sensitivity to defocus. We propose two formulations, one based on our previous work with the FI metric and the other based on a new minimization-maximization (minimax) formulation.

#### 3.1. Fisher Information Based Optimization

In previous work<sup>4</sup> we have proposed a metric based formally on the concept of Fisher information (FI) used in statistical estimation theory<sup>12</sup> to measure sensitivity to defocus. FI has been studied extensively over the past several decades, it has also been previously discussed in the context of estimation of a variety of object parameters from noisy image data, including the estimation of an object when its range is unknown.<sup>13</sup>

As before,<sup>4</sup> we consider odd-parity phase masks for which the resulting PSFs contain no odd powers of the defocus parameter  $\tau$ . Namely we consider phase functions  $\phi_\tau(\mathbf{x})$  of the form (1) with  $\theta(\mathbf{x})$  given by

$$\theta(\mathbf{x}) = a_1(x_1^3 + x_2^3) + a_2(x^2y + y^2x). \quad (11)$$

The FI metric uses the full PSF, rather than just its on-axis value.<sup>3</sup> The FI metric is of the form,

$$J_{FI}(\mathbf{a}) = \int_{-\tau_0}^{\tau_0} [J_I(\mathbf{a})]^2 d\tau, \quad (12)$$

where  $\mathbf{a} = (a_1, a_2)$  and  $(-\tau_0, \tau_0)$  denotes the (symmetric) range of defocus parameters of interest for the physical problem at hand.  $J_I(\mathbf{a})$  is given by

$$J_I(\mathbf{a}) = \iint \frac{1}{h(\boldsymbol{\omega}; \phi_\tau)} \left[ \frac{\partial h(\boldsymbol{\omega}; \phi_\tau)}{\partial \tau} \right]^2 d\omega_1 d\omega_2. \quad (13)$$

See Prasad et al<sup>4</sup> for more details regarding the FI metric.

We consider the following metric to measure restorability for a range of defocus parameters,

$$J_R(\mathbf{a}) = \int_{-\tau_0}^{\tau_0} r_\tau(\mathbf{a}) d\tau = \sum_{i=1}^{n^2} \int_{-\tau_0}^{\tau_0} \sigma_i(\tau, \mathbf{a}) d\tau. \quad (14)$$

Due to the trade-off between restorability and insensitivity to defocus, we propose the following joint minimization problem

$$\min_{\mathbf{a}} [J_{FI}(\mathbf{a}) - \lambda J_R(\mathbf{a})], \quad (15)$$

where  $\lambda$  is a control parameter that balances this trade-off.

### 3.2. A Minimax Problem

Our second formulation is aimed at maximizing restorability over a range of defocus parameters. The problem can be posed as a minimization-maximization problem by taking the negative of the sum of singular values,

$$\min_{\mathbf{a}} \max_{-\tau_0 < \tau < \tau_0} - \sum_{i=1}^{n^2} \sigma_i(\tau, \mathbf{a}) \quad (16)$$

where  $\mathbf{a}$  is a vector containing the coefficients of the pupil mask function, as before. An equivalent problem can be posed in terms of the MTF,

$$\min_{\mathbf{a}} \max_{-\tau_0 < \tau < \tau_0} - \iint M(\mathbf{u}, \phi_\tau, \mathbf{a}) dudv, \quad (17)$$

where the notation  $M(\mathbf{u}, \phi_\tau, \mathbf{a})$  emphasizes the dependence of the MTF on the coefficient vector  $\mathbf{a}$ . Here, we consider phase functions  $\phi_\tau(\mathbf{x})$  with pupil mask functions  $\theta(\mathbf{x})$  given by

$$\theta(\mathbf{x}) = a_1(x^3 + y^3) + a_2(x^2y + y^2x), \quad \mathbf{a} = (a_1, a_2) \quad (18)$$

$$\theta(\mathbf{x}) = a_1(x^3 + y^3) + a_2(x^2y + y^2x) + a_3(x^4 + y^4), \quad \mathbf{a} = (a_1, a_2, a_3) \quad (19)$$

$$\theta(\mathbf{x}) = \sum_{j=5}^{10} a_{j-4} Z_j(\mathbf{x}), \quad \mathbf{a} = (a_1, \dots, a_6), \quad (20)$$

where  $Z_j(\mathbf{x})$  are Zernike polynomials.<sup>3</sup>

## 4. COMPUTATIONAL RESULTS

In this section we present details of FI-based optimization for the symmetric mixed cubic pupil masks of the form (11) as well as of minimax-based optimization for the pupil masks specified by (18-20). Our computed phase mask designs are tested using a computer simulation software system developed by the authors. The simulator models a parabolic cone-shaped object surrounded by a set of wings arranged in a spiral at equal angles and linearly progressive distances away from a reference plane coincident with the center point. Each point in the object is blurred by a spatially varying PSF which models the appropriate defocus according to the distance from that point to the reference plane. Figure 3 illustrates the effect of noise-free spatially variant defocus. For comparison, a theoretical blur-free perspective projection of the object is also shown on the left.

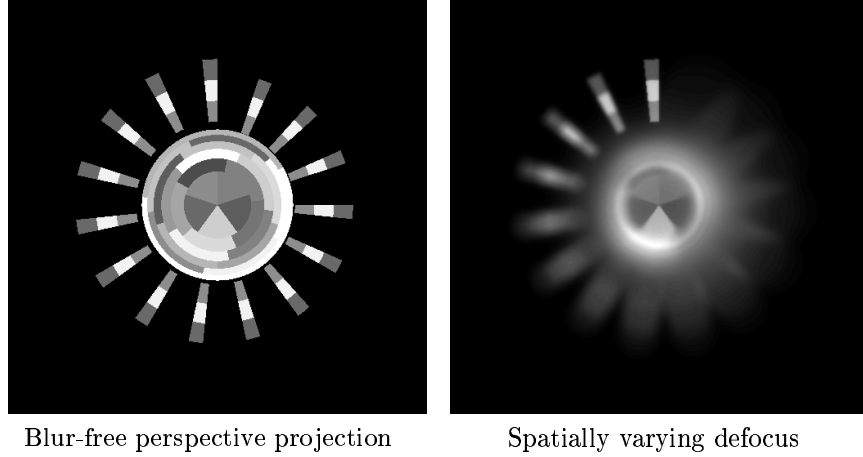


**Figure 3.** Simulated Parabolic Cone Shaped Object.

#### 4.1. Fisher Information Based Optimization

As in previous work, we employ a Monte-Carlo type technique for global optimization. Uniformly random starting points were chosen in the region  $[-100, 100] \times [-100, 100]$ , and the Levenberg-Marquardt method was applied to find a corresponding local minimum of the objective function (15) for each starting point. We set  $\lambda = 0.0625$  to emphasize the relative importance of the insensitivity to defocus term for the problem at hand. The term  $J_{FI}$  in (15) is computed using a simple quadrature rule over the range  $[-19, 19]$ . For the pupil mask function specified by (11), the optimal solution found is given by

$$\begin{bmatrix} a_1 \\ a_2 \end{bmatrix} = \begin{bmatrix} -66.9442 \\ 199.8548 \end{bmatrix}, \quad (21)$$

i.e. the pupil mask is given by the function:

$$\theta(\mathbf{x}) = -66.9442(x_1^3 + x_2^3) + 199.8548(x^2y + y^2x). \quad (22)$$

We tested the overall performance of our FI-based optimized phase mask using the simulated parabolic cone-shaped object shown in Figure 3. The simulation software integrates the pupil phase mask, as given by (21), into the blurring process. The resulting intermediate phase encoded image is shown in the left side of Figure 4. Notice the excellent spatial invariance to defocus exhibited by the intermediate image compared to the original spatially varying defocus blur of Figure 3. This intermediate image, which contains a signal-to-noise ratio of 100, was then digitally restored using the PSF (center) and a conjugate gradient type algorithm. The resulting restored image is shown on the right side of Figure 4. All images are of size  $1024 \times 1024$ .

#### 4.2. Minimax Based Optimization

The minimax problem stated in Eq. (16) was solved using the Matlab optimization toolbox. In particular, we used the `fminimax` function. As in the previous formulation, we employed a Monte-Carlo type technique for global optimization. Starting points were chosen in a uniformly random fashion in the region  $[-100, 100] \times [-100, 100]$ . The range  $[-19, 19]$  was again chosen for  $\tau$ .

For the pupil mask function specified by (18), the optimal solution found is given by the coefficients

$$\begin{bmatrix} a_1 \\ a_2 \end{bmatrix} = \begin{bmatrix} -57.1649 \\ -31.7527 \end{bmatrix}, \quad (23)$$

i.e. the pupil phase mask is given by the function:

$$\theta(\mathbf{x}) = -57.1649(x_1^3 + x_2^3) - 31.7527(x^2y + y^2x). \quad (24)$$

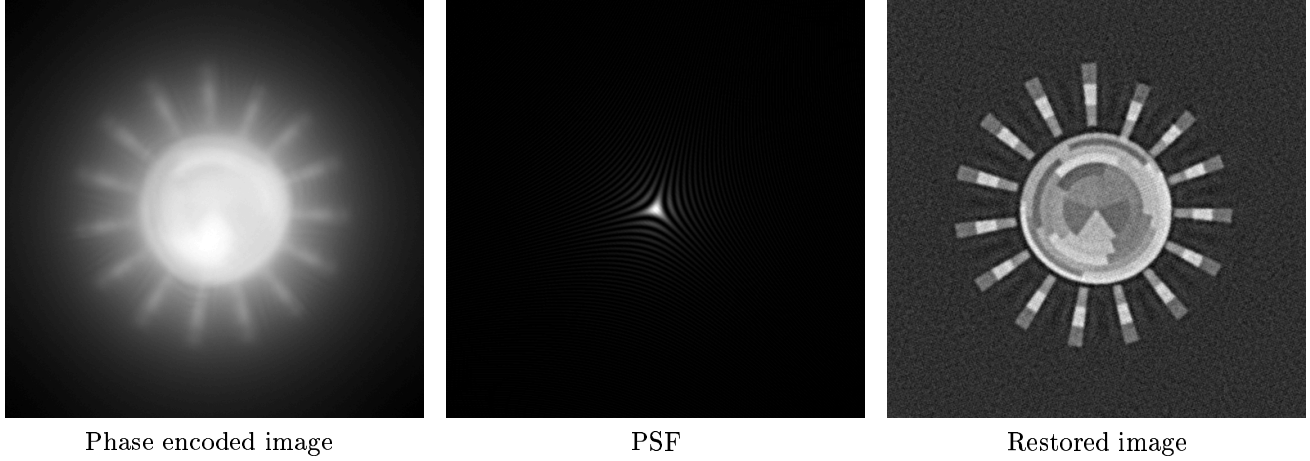


**Figure 4.** The phase-encoded blurred image, the PSF, and the restored image for the FI-optimized phase mask specified by (22).

The performance of this pupil phase mask is illustrated in Figure 5. In this case, the PSF resembles strongly that of the original cubic phase mask. Notice however the artifacts present in the intermediate phase encoded image which are also characteristic of the original cubic phase mask.

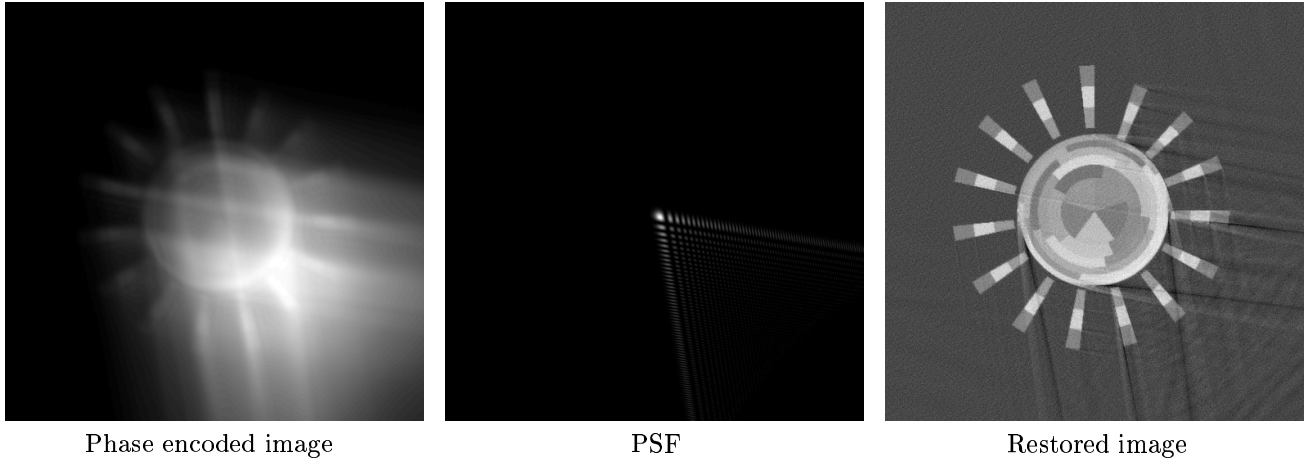


**Figure 5.** The phase-encoded blurred image, the PSF, and the restored image for the minimax-optimized phase mask specified by (24).

For the pupil mask function specified by (19), the optimal solution found is given by the coefficients

$$\begin{bmatrix} a_1 \\ a_2 \\ a_3 \end{bmatrix} = \begin{bmatrix} 15.2029 \\ -97.1492 \\ 9.9951 \end{bmatrix}, \quad (25)$$

i.e. the pupil mask is given by the function:

$$\theta(\mathbf{x}) = 15.2029(x_1^3 + x_2^3) - 97.1592(x^2y + y^2x) + 9.9951(x^4 + y^4). \quad (26)$$

The performance of this pupil phase mask is illustrated in Figure 6. The PSF resulting from this phase masks resembles that from our FI-based optimized phase mask. Notice however that the object suffers from a slightly stronger geometric distortion.

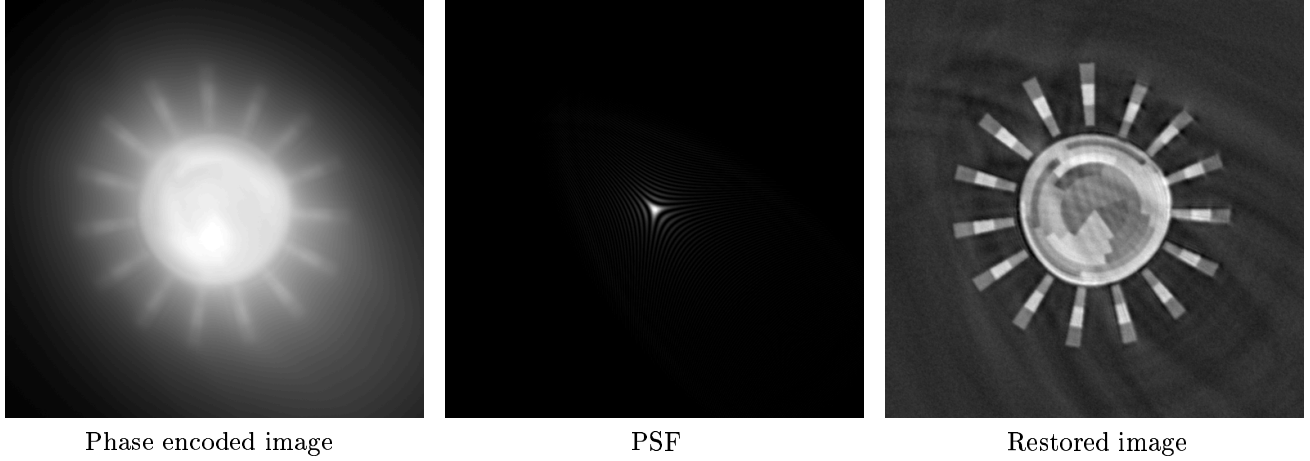


**Figure 6.** The phase-encoded blurred image, the PSF, and the restored image for the minimax-optimized phase mask specified by (26).

Finally, for the Zernike-based pupil mask specified by (20), the optimal solution found is given by the coefficients

$$\begin{bmatrix} a_1 \\ a_2 \\ a_3 \\ a_4 \\ a_5 \\ a_6 \end{bmatrix} = \begin{bmatrix} 12.4824 \\ 4.9494 \\ 10.4487 \\ 10.7163 \\ 8.6224 \\ 10.6960 \end{bmatrix}. \quad (27)$$

The performance of this pupil phase mask is illustrated in Figure 7. The shape of the PSF is similar to that encountered in our previous work using Zernike polynomials.<sup>3</sup>

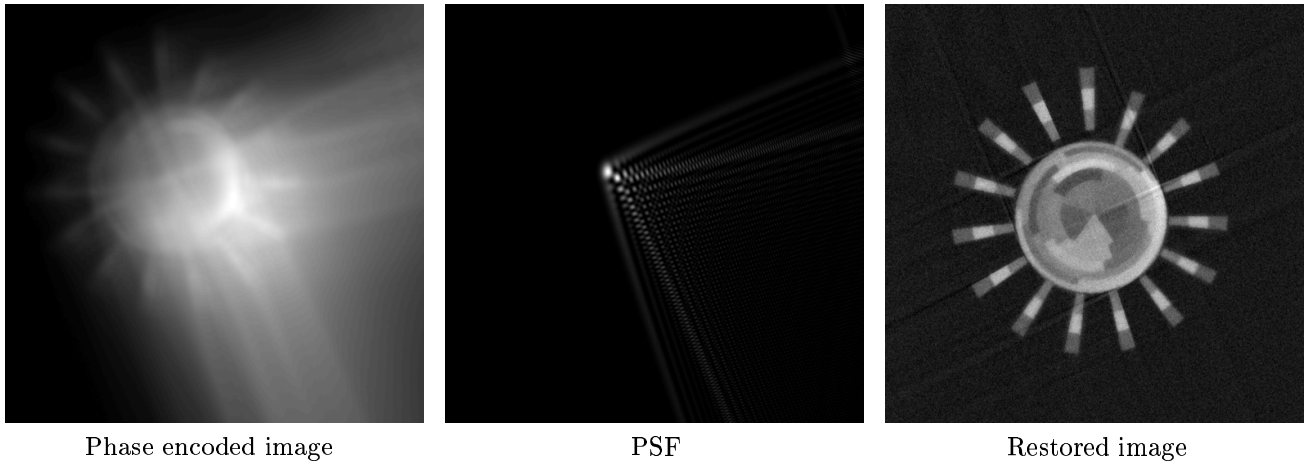


**Figure 7.** The phase-encoded blurred image, the PSF, and the restored image for the minimax-optimized Zernike phase mask specified by the coefficients (27).

## 5. FINAL REMARKS

In this paper we have examined the influence that a phase mask has on the incoming wavefront and how it subsequently affects restorability. We have also explored the design of optical masks for removing defocus-related aberrations and for maximizing restorability and information in recorded images. Two optimization

formulations were proposed, one based on our previous work with the Fisher information metric and the other based on a new minimization-maximization formulation. In the first formulation, a joint minimization problem was solved where a control parameter is employed to balance the trade-off between restorability and insensitivity to defocus. In the second formulation, we looked for phase mask function parameters that maximize the smallest sum of the singular values over an appropriate defocus range. This latter optimization approach corresponds to making the MTF insensitive to defocus over the defocus range.

## 6. ACKNOWLEDGMENT

The authors gratefully acknowledge funding support from the Air Force Office of Scientific Research under grants FA9620-01-1-0321, FA49620-02-1-0107, and FA49620-03-1-0215 and from the Army Research Office under grant DAAD19-00-1-0540. The authors also wish to thank Professor Curt Vogel from Montana State University for suggesting investigation of the minimax formulation. This research was carried out by the authors while visiting the Maui Scientific Research Center (MSRC) in Maui, HI, during the month of June, 2003.

## REFERENCES

1. W. T. Cathey and E. R. Dowski, "New paradigm for imaging systems," *Applied Optics* **41**(29), pp. 6080–6092, 2002.
2. E. R. Dowski and W. T. Cathey, "Extended depth of field through wavefront coding," *Applied Optics* **34**, pp. 1859–1866, 1995.
3. S. Prasad, T. Torgersen, V. Pauca, and R. Plemmons, "Integrated optics systems for image quality control," in *Proc. 2002 AMOS Technical Conference*, (Maui, HI), Sept. 2002.
4. S. Prasad, T. Torgersen, V. Pauca, R. Plemmons, and J. van der Gracht, "Engineering the pupil phase to improve image quality," in *Proc. SPIE AeroSense 2003*, 2003.
5. G. Golub and C. V. Loan, *Matrix Computations*, The Johns Hopkins University Press, Baltimore, MD, second ed., 1989.
6. M. Bertero and P. Boccacci, *Introduction to Inverse Problems in Imaging*, Institute of Physics Publishing, Ltd., London, 1998.
7. H. Engl, M. Hanke, and A. Neubauer, *Regularization of Inverse Problems*, Kluwer Academic Publishers, The Netherlands, 1996.
8. M. Hanke and P. C. Hansen, "Regularization methods for large-scale problems," *Surveys on Mathematics for Industry* **3**, pp. 253–315, 1993.
9. Goodman, *Introduction to Fourier Optics*, McGraw-Hill, second ed., 1996.
10. J. van der Gracht and G. W. Euliss, "Information-optimized extended depth-of-field imaging systems," in *Visual Information Processing X*, (4388), pp. 103–112, Proc. SPIE, 2001.
11. M. Hanke, J. Nagy, and R. Plemmons, "Preconditioned iterative regularization for ill-posed problems," *Numerical Linear Algebra and Scientific Computing*, pp. 141–163, 1993.
12. H. V. Trees, *Detection, Estimation, and Modulation Theory*, Wiley, 1968.
13. E. R. Dowski, "An information theoretic approach to incoherent information processing systems," in *Signal Recovery and Synthesis, OSA Technical Digest Series* **11**, pp. 106–108, Optical Society of America, 1995.